On the Impact of Ground Sound

Ante Qu and Doug L. James
Stanford University

The 22nd International Conference on Digital Audio Effects
2-6 September, 2019

Introduction

Many sound synthesis examples in animation model moving objects impacting the ground. During object-ground collisions, three types of sound are emitted:

- Object emits ringing sound from resonant modes
- Object emits a transient acceleration noise upon impact
- Ground emits a transient sound upon impact

Previous works [3][4][5] model the first two sounds and omit the third. Through physical simulation, we study the relative importance of the ground sound. Our work:

- Studies how material properties affect ground sound relevance
- Proposes an interactive method to synthesize ground sound
- Proposes an "acoustic shader" for finite-difference time-domain (FDTD) simulations to incorporate ground sound

Background: Ground Vibration Model

We model the ground surface vibration by solving Lamb's problem, and then we use it to drive sound propagation into the air.

Lamb's problem statement: Given an elastic halfspace (the ground), find the surface displacement (un(r,t)) in response to an instantaneous point load (f(t)).

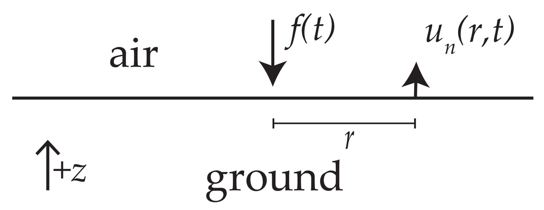

Pekeris[12] derived an analytical expression for the displacement. Unfortunately, it has a singularity at each wavefront. In this figure, the solution at 1 m away is in blue, while our temporal regularization is labeled in the other colors.

The final vertical displacement response $u_n(r,t)$ is the following:

$$u_n(r,t) = \frac{1-\nu}{2\pi\mu r}\begin{cases} 0 & \tau \le a, \\ \frac{1}{2}\left(1 - \sum_{j=1}^{3} \frac{A_j}{\sqrt{\tau^2-\kappa_j^2}}\right), & a < \tau < 1, \\ 1 - \frac{A_1}{\sqrt{\tau^2-\gamma^2}}, & 1 \le \tau < \gamma, \\ 1 & \tau \ge \gamma, \end{cases}$$

where κ_1, κ_2, κ_3 are the complex roots to the following:

$$16(1-a^2)\kappa^6 - 8(3-2a^2)\kappa^4 + 8\kappa^2 - 1 = 0,$$

$$\tau = \frac{c_s t}{r} \qquad a = \frac{c_s}{c_p} \qquad \gamma = \kappa_1,$$

$$A_j = \frac{(\kappa_j^2 - \frac{1}{2})^2\sqrt{a^2-\kappa_j^2}}{(\kappa_j^2-\kappa_i^2)(\kappa_j^2-\kappa_k^2)}, i \ne j \ne k.$$

Surface Displacement vs Time

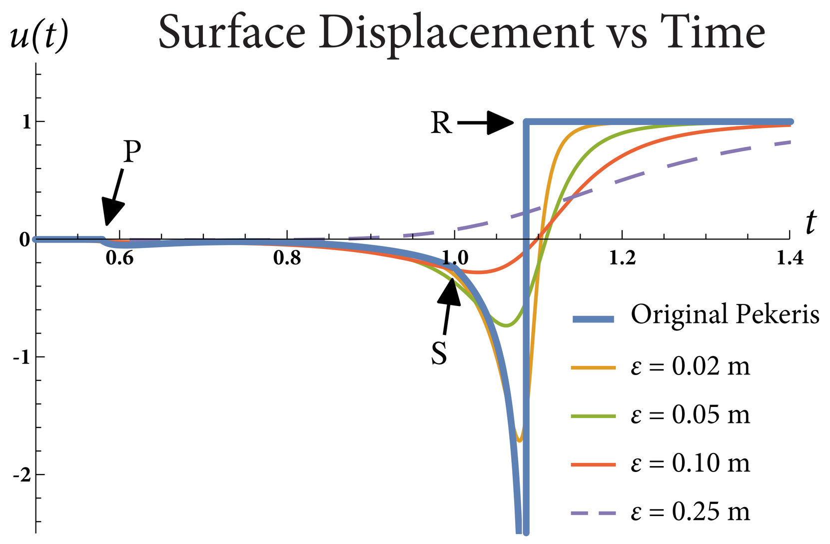

References

[3] Changxi Zheng and Doug L James, "Rigid-body fracture sound with precomputed soundbanks," in *ACM Transactions on Graphics.* ACM, 2010, vol. 29, p. 69.
[4] Changxi Zheng and Doug L James, "Toward high-quality modal contact sound," in *ACM Transactions on Graphics.* ACM, 2011, vol. 30, p. 38.
[5] Sota Nishiguchi and Katunobu Itou, "Modeling and rendering for virtual dropping sound based on physical model of rigid body," *Proc. of the 21st Int. Conf. on Digital Audio Effects (DAFx-18),* 2018.
[9] Jui-Hsien Wang, Ante Qu, Timothy R Langlois, and Doug L James, "Toward wave-based sound synthesis for computer animation," *ACM Transactions on Graphics.* ACM, 2018, vol. 37, no. 4, pp. 109.
[12] CL Pekeris, "The seismic surface pulse," *Proc. of the natl. academy of sciences of the United States of America,* vol. 41, no. 7, pp. 469, 1955.
[19] Marshall Long, "3 - human perception and reaction to sound," in *Architectural Acoustics (Second Edition),* pp. 81 – 127. Academic Press, Boston, 2014.

Method

Temporal Regularization: To smooth the singularities, we convolve the solution in time with a fourth-order smoothed delta (f_ϵ):

$$g_\epsilon(t) = \frac{c_s\epsilon}{\pi(c_s^2t^2+\epsilon^2)}; \qquad (8)$$

$$f_\epsilon(t) = 2g_\epsilon(t) - g_{2\epsilon}(t). \qquad (9)$$

We chose f_ϵ so that:

- It approximates a delta as ε → 0,
- It approximates the Hertzian half-sine contact force profile,
- It is smooth enough to eliminate the singularities, and
- The final result is a closed-form expression, for quick evaluation.

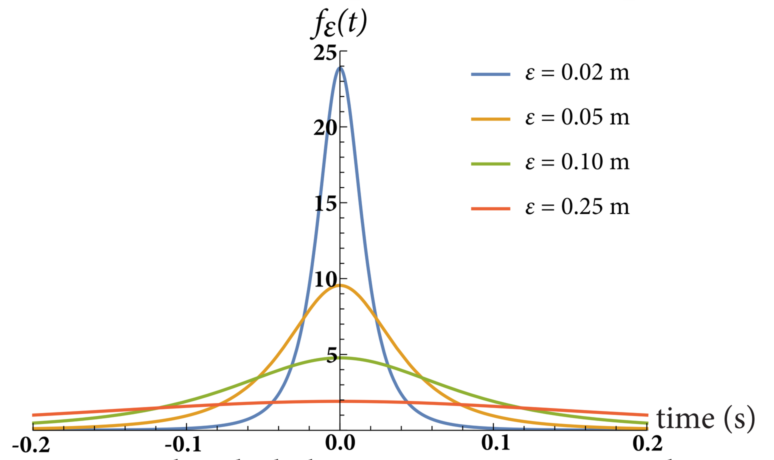

Impulse Profile: Our smoothed delta approximates the Hertz half-sine contact force, setting epsilon based on the contact timescale:

$$4\epsilon = c_s t_c = 2.87 c_s \left(\frac{m^2}{a_0 E^{*2} v_n}\right)^{1/5}, \qquad (11)$$

where a_0, m, E^*, J, v_n are the object's local radius of curvature, mass, effective stiffness, impulse, and normal impact velocity.

Ground Sound Synthesis: We use the Rayleigh Integral (Eq 12) for direct sound synthesis in our material properties studies, and we add our acoustic shader to the FDTD wavesolver in [9] for animation scenarios.

$$p(\mathbf{r}, z, t) = \rho_0 \int_{\mathbb{R}^2} \frac{a_\epsilon(\mathbf{r}', t - R'/c_0)}{2\pi R'} d\mathbf{r}', \qquad (12)$$

Results: Validation and Sound Synthesis

Model Validation: The regularized solution converges to the ideal as ε → 0.

Sound Synthesis: Ideal ball expression:

$$p(\mathbf{r},t) = \frac{\rho_0 a_0^3 \cos(\theta)}{2}\left(-\frac{a(t-\frac{r-a_0}{c_0})}{r^2} + \frac{\frac{da}{dt}(t-\frac{r-a_0}{c_0})}{c_0 r}\right) \qquad (16)$$

Steel Ball (Ideal), Wood Floor (Rayleigh)

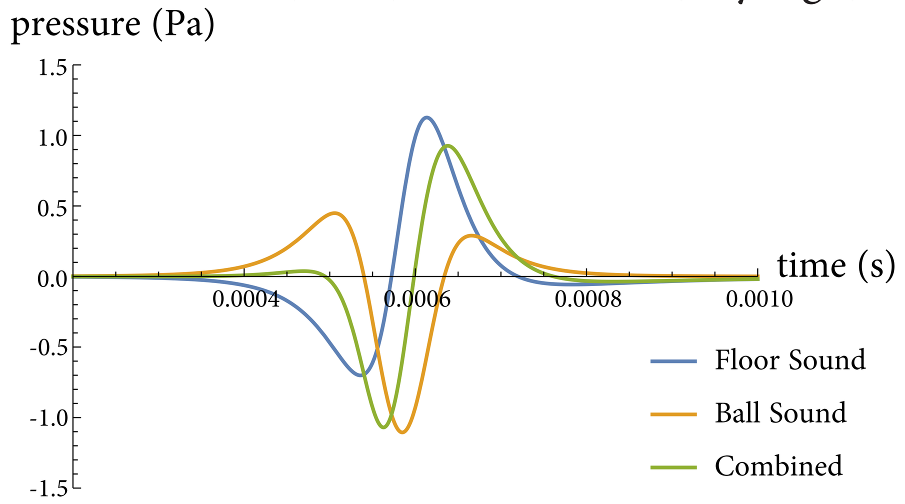

Steel Ball, Concrete Ground (FDTD)

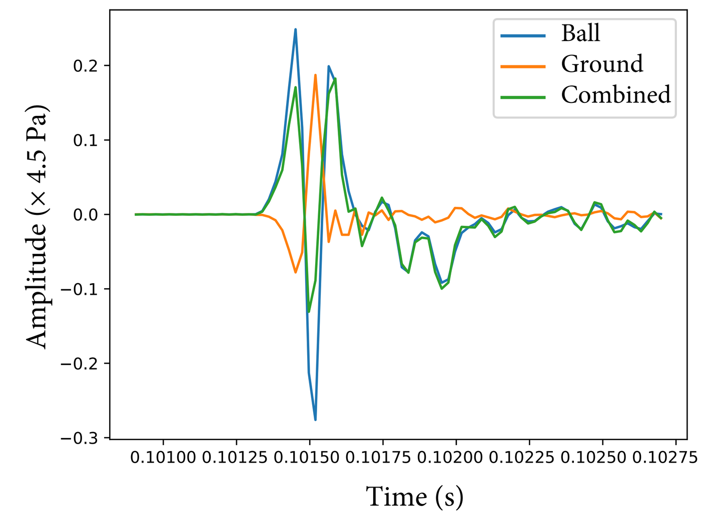

Acknowledgements

We acknowledge support from the National Science Foundation (DGE-1656518), the Toyota Research Institute, and Google Cloud Platform compute resources.

Results: Material and Listening Angle Dependance

Consider a ball dropped from a fixed height onto the ground.

- Listening Angle (θ): Observe in this plot that overhead listening angles receive more ball sound, while lower elevation angles receive more ground sound.

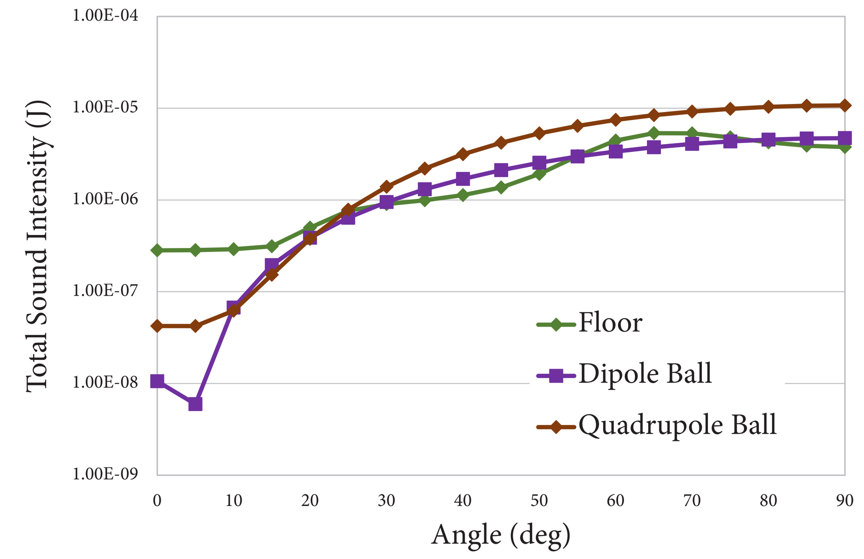

Paper and examples online at graphics.stanford.edu/papers/ground/

- Ball density (ρ_b), ground stiffness (E_f): For fixed initial drop height, the ground sound amplitude is proportional to ρ_b/E_f, while the ball sound is unaffected. See
- Ground speed of shear waves (c_s): The ball sound does not depend on c_s, while the ground amplitude increases linearly with c_s until a knee threshold c_k.

Theoretical Relative Intensities (dB) of Ground to Ball Sound, Measured Overhead

ball \ ground	Steel	Ceramics	Granite	Concrete	Wood	Plastic	Soil	Wax
Steel	-30.25	-21.30	-18.94	-11.83	-6.12	4.15	19.06	19.58
Ceramics	-39.63	-30.69	-28.33	-21.22	-15.51	-5.23	9.68	10.19
Granite	-39.73	-30.78	-28.43	-21.32	-15.60	-5.33	9.58	10.10
Concrete	-41.21	-32.27	-29.91	-22.80	-17.09	-6.81	8.09	8.61
Wood	-50.76	-41.81	-39.46	-32.34	-26.63	-16.36	-1.45	-0.93
Plastic	-47.67	-38.73	-36.37	-29.26	-23.55	-13.27	1.64	2.15
Soil	-45.65	-36.71	-34.35	-27.24	-21.53	-11.25	3.65	4.17
Wax	-50.35	-41.41	-39.05	-31.94	-26.22	-15.95	-1.04	-0.53

Positive values indicate the ground was louder than the ball (teal). Other values above the most sensitive JND level of -13 dB [19] are in light orange.

Theoretical Relative Intensities (dB) of Ground to Ball Sound, 5° above Ground

ball \ ground	Steel	Ceramics	Granite	Concrete	Wood	Plastic	Soil	Wax
Steel	-17.43	-8.48	-6.13	0.99	6.70	16.97	31.88	32.40
Ceramics	-26.81	-17.87	-15.51	-8.40	-2.69	7.59	22.49	23.01
Granite	-26.91	-17.97	-15.61	-8.50	-2.78	7.49	22.40	22.91
Concrete	-28.40	-19.45	-17.10	-9.98	-4.27	6.00	20.91	21.43
Wood	-37.94	-29.00	-26.64	-19.53	-13.81	-3.54	11.37	11.88
Plastic	-34.85	-25.91	-23.55	-16.44	-10.73	-0.45	14.45	14.97
Soil	-32.83	-23.89	-21.53	-14.42	-8.71	1.57	16.47	16.99
Wax	-37.53	-28.59	-26.23	-19.12	-13.41	-3.13	11.77	12.29

Discussion and Conclusion

We found the following three properties affect ground sound importance:

- Object density (denser objects → louder ground)
- Ground stiffness (softer grounds → louder ground sound)
- Listening angle (lower elevation angles → louder ground)

This is only important when the object's modal ringing noise, which is louder in large objects, is not audible.

Future work directions:

- Model resonant modes in floors with finite depth and buildings
- Regularize the response to tangential forces incurred by contact friction
- Derive an analytical approximation for the final sound based on listening angle